NeuroImage: Clinical 38 (2023) 103390

Contents lists available at ScienceDirect

NeuroImage: Clinical

journal homepage: www.elsevier.com/locate/ynicl

Abnormal cerebral hemodynamics and blood-brain barrier permeability detected with perfusion MRI in systemic lupus erythematosus patients

T. Salomonsson [a], T. Rumetshofer [a,b], A. Jönsen [c], A.A. Bengtsson [c], K.A. Zervides [c], P. Nilsson [d], M. Knutsson [a], R. Wirestam [e], J. Lätt [h], L. Knutsson [e,f,g,1], P.C. Sundgren [a,h,i,*,1]

[a] Department of Clinical Sciences/Radiology, Lund University, Lund, Sweden
[b] Department of Clinical Sciences/Division of Logopedics, Phoniatrics and Audiology, Lund University, Lund, Sweden
[c] Department of Clinical Sciences Lund/Rheumatology, Lund University, Skåne University Hospital, Lund, Sweden
[d] Department of Clinical Sciences Lund/Neurology, Lund University, Skåne University Hospital, Lund, Sweden
[e] Department of Medical Radiation Physics, Lund University, Lund, Sweden
[f] Russell H. Morgan Department of Radiology and Radiological Science, Johns Hopkins University School of Medicine, Baltimore, MD, United States
[g] F.M. Kirby Research Center for Functional Brain Imaging, Kennedy Krieger Institute, Baltimore, MD, United States
[h] Department of Medical Imaging and Physiology, Skåne University Hospital, Lund, Sweden
[i] Lund University Bioimaging Center, Lund University, Lund, Sweden

ARTICLE INFO

Keywords:
Dynamic susceptibility contrast
White matter hyperintensities
Systemic lupus erythematosus
Cerebral perfusion
Blood-brain-barrier

ABSTRACT

Objective: Dynamic susceptibility contrast (DSC) magnetic resonance imaging (MRI) has previously shown alterations in cerebral perfusion in patients with systemic lupus erythematosus (SLE). However, the results have been inconsistent, in particular regarding neuropsychiatric (NP) SLE. Thus, we investigated perfusion-based measures in different brain regions in SLE patients with and without NP involvement, and additionally, in white matter hyperintensities (WMHs), the most common MRI pathology in SLE patients.

Materials and methods: We included 3 T MRI images (conventional and DSC) from 64 female SLE patients and 19 healthy controls (HC). Three different NPSLE attribution models were used: the Systemic Lupus International Collaborating Clinics (SLICC) A model (13 patients), the SLICC B model (19 patients), and the American College of Rheumatology (ACR) case definitions for NPSLE (38 patients). Normalized cerebral blood flow (CBF), cerebral blood volume (CBV) and mean transit time (MTT) were calculated in 26 manually drawn regions of interest and compared between SLE patients and HC, and between NPSLE and non-NPSLE patients. Additionally, normalized CBF, CBV and MTT, as well as absolute values of the blood-brain barrier leakage parameter (K_2) were investigated in WMHs compared to normal appearing white matter (NAWM) in the SLE patients.

Results: After correction for multiple comparisons, the most prevalent finding was a bilateral significant decrease in MTT in SLE patients compared to HC in the hypothalamus, putamen, right posterior thalamus and right anterior insula. Significant decreases in SLE compared to HC were also found for CBF in the pons, and for CBV in the bilateral putamen and posterior thalamus. Significant increases were found for CBF in the posterior corpus callosum and for CBV in the anterior corpus callosum. Similar patterns were found for both NPSLE and non-NPSLE patients for all attributional models compared to HC. However, no significant perfusion differences were revealed between NPSLE and non-NPSLE patients regardless of attribution model. The WMHs in SLE patients showed a significant increase in all perfusion-based metrics (CBF, CBV, MTT and K_2) compared to NAWM.

Conclusion: Our study revealed perfusion differences in several brain regions in SLE patients compared to HC, independently of NP involvement. Furthermore, increased K_2 in WMHs compared to NAWM may indicate blood-brain barrier dysfunction in SLE patients. We conclude that our results show a robust cerebral perfusion, independent from the different NP attribution models, and provide insight into potential BBB dysfunction and altered vascular properties of WMHs in female SLE patients. Despite SLE being most prevalent in females, a generalization of our conclusions should be avoided, and future studies including all sexes are needed.

* Corresponding author at: Department of Clinical Sciences/Radiology, Lund University Bioimaging Center, Lund University, Department of Medical Imaging and Physiology, Skåne University Hospital, Lund SE-221 85, Sweden.
E-mail address: pia.sundgren@med.lu.se (P.C. Sundgren).
[1] Shared last authors.

https://doi.org/10.1016/j.nicl.2023.103390
Received 18 January 2023; Received in revised form 24 March 2023; Accepted 25 March 2023
Available online 28 March 2023

1. Introduction

Neuropsychiatric (NP) involvement includes several manifestations of the nervous system in systemic lupus erythematosus (SLE), estimated to occur in more than half of all SLE patients, with a prevalence varying between 12 and 95 % (Unterman et al., 2011). Neuropsychiatric SLE (NPSLE) patients often require more intense treatment with glucocorticoids and cytostatic drugs, and report increased fatigue and reduced quality of life compared to SLE patients without attributable NP events (non-NPSLE) (Hanly et al., 2004). The most prevalent central nervous system (CNS) manifestations associated with NPSLE are diffuse, including headaches, mood disorders and cognitive dysfunction, each having an estimated prevalence of at least 20 % (Unterman et al., 2011). Other common CNS manifestations have more focal character, such as cerebrovascular disease and seizures (Unterman et al., 2011). Postulated pathophysiologies contributing to NPSLE consist of mainly ischemic or autoimmune processes, including systemic and intrathecal autoantibody production, focal or general vascular pathology, as well as disruption of the blood-brain barrier (BBB) (Nikolopoulos et al., 2019; Stock et al., 2017; Ota et al., 2022). The imaging characteristics for each of these mechanisms differ, although features may overlap (Ota et al., 2022).

When using conventional brain magnetic resonance imaging (MRI), the most common findings are focal white matter hyperintensities (WMHs) (reported in up to 60 % of NPSLE patients) and cerebral atrophy (up to 43 %) (Ota et al., 2022; Jennings et al., 2004; Luyendijk et al., 2011). However, these abnormalities are non-specific and a considerable number of NPSLE patients (34–42 %) exhibit normal findings on conventional MRI (Ota et al., 2022; Jennings et al., 2004; Luyendijk et al., 2011). Several factors have been proposed as possible mechanisms contributing to WMH load, including inflammation, ischemia, increased BBB permeability, age, disease activity, vasculitis, small vessel disease as well as demyelination and autoimmune antibody-mediated mechanisms (Ota et al., 2022; Luyendijk et al., 2011; Shaharir et al., 2018).

Previous perfusion MRI studies with dynamic susceptibility contrast (DSC) and arterial spin labeling (ASL) have demonstrated mainly regional or asymmetrically reduced perfusion in NPSLE patients (Borrelli et al., 2003; Papadaki et al., 2018; Papadaki et al., 2019; Zhuo et al., 2020; Jia et al., 2019). Hypoperfusion has been found in the thalami, centra semiovale, frontal lobes, corpus callosum and cerebellum in NPSLE compared to non-NPSLE patients (Papadaki et al., 2018; Zhuo et al., 2020; Jia et al., 2019). Normal appearing white matter (NAWM), thalami, basal ganglia, dorsolateral and ventromedial prefrontal cortex have shown decreased perfusion in NPSLE patients compared to healthy controls (HC) (Papadaki et al., 2018; Papadaki et al., 2019; Zhuo et al., 2020). Increased perfusion has been found in non-NPSLE patients overall and regionally in the hypothalami, posterior thalami, cingulate gyrus and cerebellum compared to HC (Zhuo et al., 2020; Gasparovic et al., 2010; Wang et al., 2012). Notably, others have found no differences in perfusion-based measures between any of the groups (Emmer et al., 2010; Zimny et al., 2014). A previous study has demonstrated an increased variability in perfusion metrics in NPSLE compared to non-NPSLE patients, which has been proposed as a possible explanation for some of the inconclusive findings (Wang et al., 2012). Additionally, research using dynamic contrast-enhanced (DCE) MRI has previously indicated that SLE patients have an increased BBB permeability compared to HC (Chi et al., 2019; Kamintsky et al., 2020).

In light of these previous MRI perfusion and permeability findings (Borrelli et al., 2003; Papadaki et al., 2018; Papadaki et al., 2019; Zhuo et al., 2020; Jia et al., 2019; Gasparovic et al., 2010; Wang et al., 2012; Emmer et al., 2010; Zimny et al., 2014; Chi et al., 2019; Kamintsky et al., 2020), the present study was conducted to further evaluate perfusion-based measures with DSC-MRI in an SLE cohort, while also investigating potential discrepancies when using different attribution models for NPSLE. Our primary aim was to investigate whether SLE patients exhibit altered patterns of cerebral perfusion compared to HC, and NPSLE compared to non-NPSLE patients, in specific predefined anatomical brain regions. We also aimed at investigating whether BBB dysfunction and altered vascular properties were present in WMH compared to NAWM in SLE patients. We applied different perfusion and permeability metrics including cerebral blood flow (CBF), cerebral blood volume (CBV), mean transit time (MTT) and the BBB leakage parameter K_2.

2. Materials and methods

2.1. Participants

This cross-sectional study included 64 female SLE patients, consecutively recruited independently of NP events or disease activity from the tertiary rheumatology outpatient clinic at Skåne University Hospital, Lund, Sweden. Each patient fulfilled at least four of the Systemic Lupus International Collaborating Clinics (SLICC) classification criteria for SLE, including at least one clinical and one immunological (Petri et al., 2012). In order to reduce study group heterogeneity, inclusion criteria were female, age between 18 and 55 years (reducing the likelihood of age-related MRI abnormalities) and right-handedness (reducing potential differences in hemisphere dominance between subjects). Exclusion criteria were any contraindication to performing MRI such as claustrophobia, pacemaker, metal implant, pregnancy or contrast agent allergy. SLE disease activity was assessed using the Systemic Lupus Erythematosus Disease Activity Index 2000 (SLEDAI-2 K) (Gladman et al., 2002 Feb) and irreversible organ damage using the SLICC/American College of Rheumatology (ACR) Damage Index (SDI) (Gladman et al., 1996).

A rheumatologist and a neurologist clinically evaluated all SLE patients regarding ongoing or history of NP events attributed to SLE, which were then defined according to the 19 case definitions published by the ACR (The American College of Rheumatology, 1999), herein stated as the “NPACR model”. A diagnosis of NPSLE required consensus between the two clinicians. The rheumatologist further classified the NPACR patients according to the attribution models SLICC A and SLICC B (Hanly et al., 2007; Hanly et al., 2008), including patients with attributable NP events within 6 months and 10 years prior to SLE diagnosis, respectively. The SLICC models excluded NP events based on contributing non-SLE factors in the NPACR model, while also excluding minor NP events commonly found among the general population: headache, anxiety, mild depression, mild cognitive dysfunction and polyneuropathy without electroneurography confirmation (Ainiala et al., 2001). Each patient had to fulfill the requirements of at least one NP manifestation according to the different attribution models to be included in the respective NPSLE group. Conversely, patients without attributable NP events were referred to as non-NPSLE.

For the comparison group, perfusion MRI data from 20 HC (10 female, 10 male) collected from a previous study (Knutsson et al., 2014) were reanalyzed and compared with the data obtained from the SLE patients. As part of that study, a neurologist evaluated the HC subjects and their medical histories were reviewed, to exclude cognitive deficits and any medications that could potentially have altered the cerebral perfusion. Additionally, conventional MRI scans were performed to rule out visible pathology in the HC group.

Written informed consent was obtained from all subjects and the project was approved by the local ethics committee (the SLE study has ethical permits 2012/254, 2012/677 and 2014/778, and the HC study has permit 2008/703).

2.2. MR imaging

The SLE cohort was examined on a 3 T MRI scanner (MAGNETOM Skyra, Siemens, Erlangen, Germany). The structural series included: axial T2-weighted fluid-attenuated inversion recovery (FLAIR) (axial plane resolution 0.7×0.7 mm^2, slice thickness 3 mm, echo time (TE) = 81 ms, repetition time (TR) = 9000 ms and inversion time (TI) = 2500

ms), and axial T1-weighted magnetization-prepared rapid gradient-echo (MPRAGE) before and after contrast agent administration (axial plane resolution 1×1 mm^2, slice thickness 1 mm, TE = 2.5 ms, TR = 1900 ms and TI = 900 ms). Perfusion weighted imaging (PWI) was performed using a DSC-MRI gradient-echo echo planar imaging (EPI) sequence with the following sequence parameters: axial plane resolution 1.72×1.72 mm^2, slice thickness 5 mm, field of view (FOV) 220×220 mm^2, image matrix 128×128, TE = 28 ms, TR = 1470 ms, 23 slices, flip angle 90° and an acquisition time of 1:53 min. A bolus (injection rate 5 ml/s) of 0.1 mmol/kg body weight gadolinium contrast agent (Dotarem®, Gothia Medical, Guerbet, France) was administered, followed by a 20 ml saline flush injected at the same rate.

The HC cohort was examined on a 3 T MRI scanner (Achieva, Philips Medical Systems, Best, The Netherlands). The structural series included: axial T2-weighted FLAIR (axial plane resolution 0.43×0.43 mm^2, slice thickness 5 mm, TE = 140 ms, TR = 12000 ms and TI = 2850 ms), and a T1-weighted Look-Locker sequence before and after contrast agent administration (axial plane resolution 1.7×1.7 mm^2, slice thickness 6 mm, TE = 3.5 ms and TR = 8.0 ms). PWI was performed using a DSC-MRI gradient-echo EPI sequence with the following sequence parameters: axial plane resolution 1.72×1.72 mm^2, slice thickness 5 mm, FOV 220×220 mm^2, image matrix 128×128, TE = 29 ms, TR = 1243 ms, 20 slices, flip angle 60° and an acquisition time of 1:30 min. A gadolinium contrast agent of 0.1 mmol/kg body weight (Dotarem®, Gothia Medical, Guerbet, Paris, France) was injected during the DSC-MRI imaging. In addition, a prebolus of 0.02 mmol/kg body weight gadolinium contrast agent (Dotarem®, Gothia Medical, Guerbet, France) preceded the DSC-MRI measurement (Knutsson et al., 2014) and was not further considered in the present study. Both bolus doses were administered at an injection rate of 5 ml/s, followed by a 20 ml saline flush at the same rate.

2.3. MRI perfusion analysis

The DSC-MRI images were processed using the software nordicICE (NordicNeuroLab, Bergen, Norway) and the perfusion processing was carried out as follows: The signal in each voxel was converted to transverse relaxation-rate change ΔR2*, and a linear relationship between ΔR2*(t) and the contrast agent concentration was assumed (Fisel et al., 1991). The CBV maps were calculated by dividing the area of the concentration time curve in each voxel with the area of the arterial input function (AIF). The CBF and MTT maps were calculated using the central volume theorem (CBF = CBV/MTT) and Zierler's area–to–height relationship after deconvolution of tissue concentration curves with the AIF using a singular value decomposition (SVD) deconvolution algorithm (Wu et al., 2003). The AIF was defined by taking the average of semi-automatically selected voxels within the branches of the middle cerebral artery (MCA) around the Sylvian fissure. The contrast agent leakage was corrected for using a linear fitting algorithm and K_2 was calculated using an estimation of the extravasation of the contrast agent by determining deviation from a 'non-leaky' reference tissue response curve (Boxerman et al., 2006).

Maps of CBF, CBV and MTT were analyzed using the in-house MATLAB R2016b (RRID:SCR_001622) software Eval GUI (developed by Markus Nilsson at Lund University, Sweden). Based on earlier findings and previously investigated areas in SLE (Borrelli et al., 2003; Papadaki et al., 2018; Papadaki et al., 2019; Zhuo et al., 2020; Jia et al., 2019; Gasparovic et al., 2010; Wang et al., 2012; Emmer et al., 2010; Zimny et al., 2014; Chi et al., 2019; Kamintsky et al., 2020), 26 regions of interest (ROIs) were placed in pons, insulae, hypothalami, nuclei caudatus, putamina, posterior thalami, corpus callosum, cingulate gyrus, frontal and parietal gray matter (GM), and frontal, parietal, temporal and occipital white matter (WM). The manually drawn ROIs were 40 pixels in size (volume 0.59 ml), except for the insula ROIs which were 20 pixels in size (volume 0.30 ml). The ROIs were manually placed by a junior colleague (TS) with guidance from a senior neuroradiologist with 30 years of experience (PCS). The FLAIR or T1-weighted images were used as anatomical reference and any signal alterations such as WMHs were avoided. Corresponding color-coded CBF maps were used to avoid ROI placement directly in the intravascular space (example shown in Fig. 1). The researchers were blinded to clinical patient information during these steps.

The values for CBF, CBV and MTT obtained from the ROIs were normalized for each subject, by dividing with the respective value of the middle cerebellar peduncle. This generated relative perfusion-based values (denoted rCBF, rCBV and rMTT), which were summarized as means with standard deviation for each ROI and compared between SLE and HC, as well as between NPSLE, non-NPSLE and HC (using the SLICC A, SLICC B and NPACR model). The differences in rCBF, rCBV and rMTT were then presented as the mean increase or decrease in percent in SLE patients relative to the values obtained in the HC group ($\%_{SLEvsHC}$ = ((SLE/HC) − 1) × 100). The same calculations were used for the NPSLE patients relative to the non-NPSLE patients ($\%_{NPSLEvsnon\text{-}NPSLE}$ = ((NPSLE/non-NPSLE) − 1) × 100), the NPSLE patients relative to the HC group ($\%_{NPSLEvsHC}$ = ((NPSLE/HC) − 1) × 100) and the non-NPSLE patients relative to the HC group ($\%_{non\text{-}NPSLEvsHC}$ = ((non-NPSLE/HC) − 1) × 100).

2.4. White matter hyperintensities

The WMH regions for each SLE patient were manually delineated in the axial FLAIR images, using the Eval GUI software tool, by two trained researchers (TS and TR) and evaluated by an experienced neuroradiologist (PCS). WMHs smaller than 0.015 ml were removed to reduce the impact of partial volume effects (PVEs) and false positives. To ensure that the segmented WMH maps overlapped correctly with the PWI images, the following preprocessing steps were applied: The FLAIR images were co-registered to PWI-space using the Linear Image Registration Tool (FLIRT) (Jenkinson and Smith, 2001; Jenkinson et al., 2002) in the FMRIB Software Library (FSL) software 5.0.10 (RRID:SCR_002823) (Smith, 2002) using sinc interpolation. The WMH maps were then transferred to PWI-space using the transformation matrices obtained from the above-mentioned FLIRT co-registration, using NearestNeighbor interpolation.

ROIs were manually placed in WMHs larger than or equal to 3 pixels in PWI-space (volume ≥0.044 ml) (example shown in Fig. 2). Two ROIs of 40 pixels each were placed in NAWM of the centra semiovale (volume 1.18 ml), as this area was located in the vicinity of the majority of the WMHs. Relative perfusion-based values (rCBF, rCBV and rMTT), normalized to the respective value of the middle cerebellar peduncle, and absolute values for K_2 were calculated for the WMHs and NAWM in the SLE cohort. The differences in rCBF, rCBV, rMTT and K_2 were then presented as the mean increase or decrease in percent in the WMHs relative to the values obtained in NAWM ($\%_{WMHvsNAWM}$ = ((WMH/NAWM) − 1) × 100). Descriptive values regarding WMH size (ml/WMH), WMH volume (ml/patient) and WMH burden (total number of measurable WMHs for each subject) were calculated using the ROIs in PWI-space. During all the above steps clinical patient information was blinded.

2.5. Statistical analysis

All statistical analyses were carried out using the Python package SciPy 1.9.1 (RRID:SCR_008058) (Virtanen et al., 2020 Mar). Each perfusion comparison was performed separately, as described below, and the same approach was used to assess differences in age between the groups. A Shapiro-Wilk test ($p < 0.05$) was used to check for normal distribution. Differences between SLE and HC were analyzed using a two-sided *t*-test or a Mann-Whitney *U* test. Comparisons between NPSLE, non-NPSLE and HC applied the SLICC A, SLICC B and NPACR models separately, using a one-way ANOVA with post-hoc Tukey HSD test or Kruskal-Wallis test with pairwise Mann-Whitney U tests. Bonferroni correction was applied to each of the following perfusion analyses

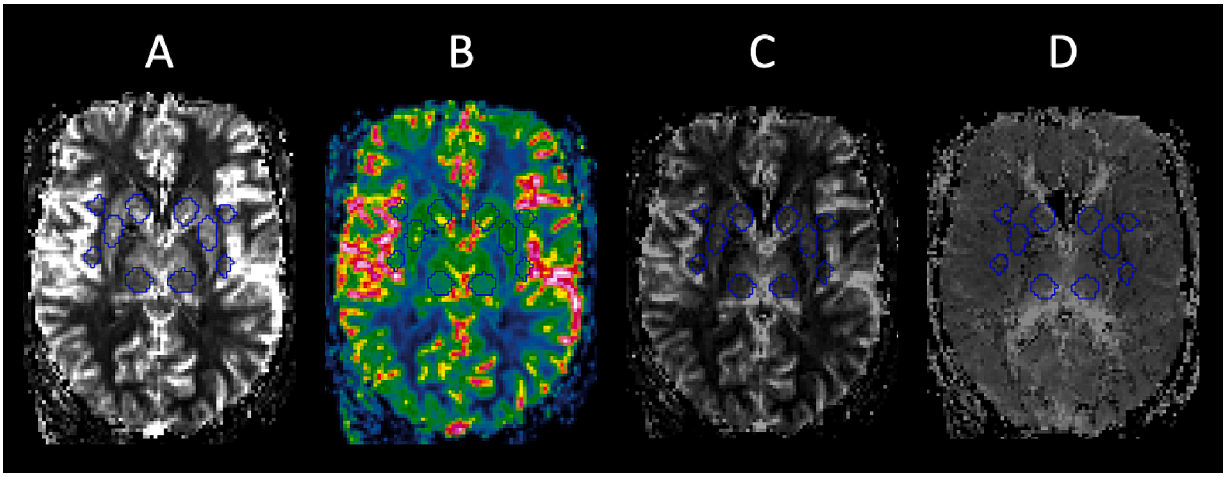

Fig. 1. Example showing ten of the 26 anatomical ROIs in an SLE patient, placed in the nuclei caudatus, putamina, posterior thalami, anterior and posterior insulae. The color-coded CBF image (B) was used to avoid pixels with high blood flow, indicating intravascular space. Relative perfusion-based parameters were extracted from the CBF (A), CBV (C) and MTT (D) maps. ROI = region of interest, SLE = systemic lupus erythematosus, CBF = cerebral blood flow, CBV = cerebral blood volume, MTT = mean transit time.

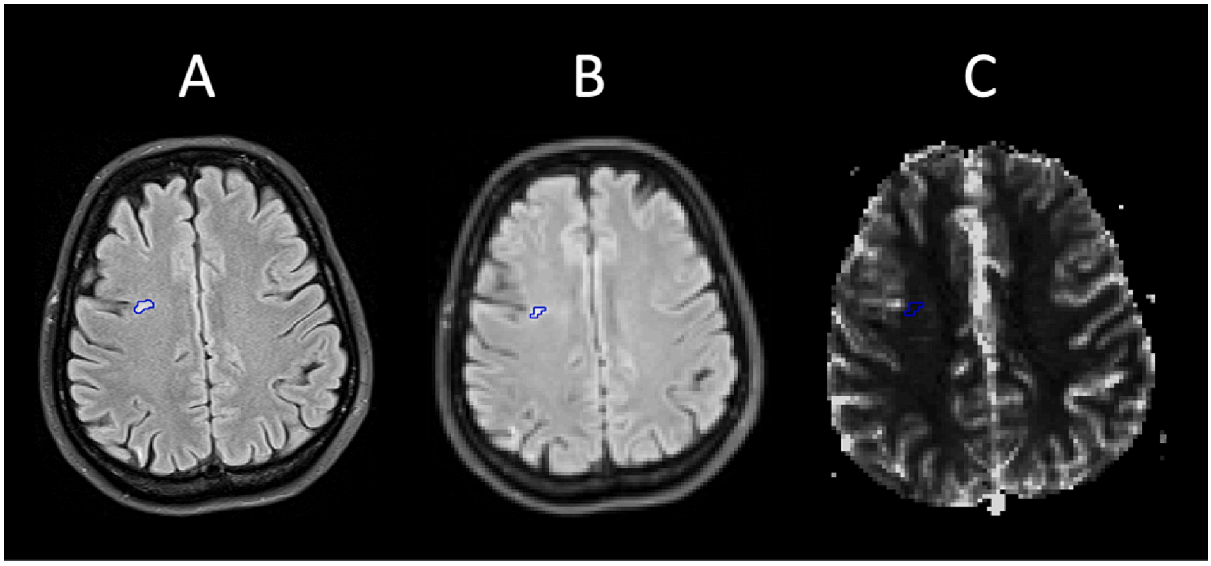

Fig. 2. One of the WMH ROIs identified by the FLAIR image (A). Co-registering the FLAIR and PWI scans (B) ensured correct ROI placement in the PWI maps (C; example for CBF). WMH = White matter hyperintensity, ROI = region of interest, FLAIR = fluid-attenuated inversion recovery, PWI = perfusion weighted imaging, CBF = cerebral blood flow.

separately to account for multiple comparisons, setting the statistical significance to $p < 0.00064$ (calculated $0.05/(26\times3)$, as each group comparison had 26 ROIs with 3 perfusion parameters (rCBF, rCBV, rMTT) each): SLE vs HC, SLICC A vs non-SLICC A vs HC, SLICC B vs non-SLICC B vs HC, NPACR vs non-NPACR vs HC. An additional analysis with only females in the HC cohort was also performed, and results are presented in the supplementary material.

WMHs in SLE were compared to NAWM with a two-sided *t*-test or a Mann-Whitney *U* test for rCBF, rCBV, rMTT and K_2. These four perfusion-based parameters were analyzed (in terms of WMH vs NAWM) for each of the following groups separately: SLE, SLICC A, SLICC B, NPACR, non-SLICC A, non-SLICC B and non-NPACR. The NPSLE and non-NPSLE WMH groups were also compared using the same statistical tests regarding age, WMH burden, WMH size and WMH volume (using the SLICC A, SLICC B and NPACR models separately).

3. Results

3.1. Clinical characteristics

An overview of the clinical characteristics of the 64 SLE patients is presented in Table 1. The median SLEDAI-2 K score was 2 (range 0–18), with 16 patients (25 %) having SLEDAI-2 K ≥4, and the median SDI score was 0 (range 0–5), with 20 patients (31 %) having SDI ≥1. The majority of the patients were treated with immunosuppressive medications such as hydroxychloroquine (80 %), prednisolone (78 %) or other disease-modifying antirheumatic drugs (DMARDs) (59 %). Due to severe hydrocephalus in one HC, the ROIs for perfusion measurements could not be placed correctly in this subject. Therefore, this HC had to be excluded, leaving 19 HCs (10 female, median age 31 years, range 25–74 years) to be included in the final analysis. There were no significant age differences between SLE and HC ($p = 0.23$) or between NPSLE, non-NPSLE and HC, regardless of attribution model (SLICC A: $p = 0.18$, SLICC B: $p = 0.46$ and NPACR: $p = 0.35$).

Table 1
Clinical characteristics of the 64 female SLE patients in this study, including current treatment and prevalence of the fulfilled SLICC classification criteria for SLE.

Clinical characteristics	
Age [years], median (range)	39 (18–52)
Disease duration [years], median (range)[a]	11 (0–26)
SLEDAI-2 K, median (range)	2 (0–18)
SDI, median (range)	0 (0–5)
Smoking, n (%)[b]	23 (36 %)
Treatment	
Hydroxychloroquine, n (%)	51 (80 %)
Other DMARDs except hydroxychloroquine, n (%)	38 (59 %)
Prednisolone, n (%)	50 (78 %)
Prednisolone daily dose [mg/day], median (range)	5 (0–25)
Antihypertensive medication, n (%)	19 (30 %)
SLICC criteria for SLE classification	
Acute cutaneous lupus, n (%)	46 (72 %)
Chronic cutaneous lupus, n (%)	16 (25 %)
Oral or nasal ulcers, n (%)	27 (42 %)
Non scarring alopecia, n (%)	23 (36 %)
Joint disease, n (%)	55 (86 %)
Serositis (%)	27 (42 %)
Renal manifestations, n (%)	24 (38 %)
Neurological manifestations, n (%)	9 (14 %)
Hemolytic anemia, n (%)	3 (5 %)
Leukopenia or lymphopenia, n (%)	39 (61 %)
Thrombocytopenia, n (%)	19 (30 %)
ANA, n (%)	63 (98 %)
Anti-dsDNA, n (%)	38 (59 %)
Anti-Sm, n (%)	11 (17 %)
aPL, n (%)[c]	20 (31 %)
Low complement, n (%)	38 (59 %)
Positive Direct Coombs test, n (%)	2 (3 %)

SLE = Systemic lupus erythematosus, SLICC = Systemic Lupus International Collaborating Clinics, SLEDAI-2 K = Systemic Lupus Erythematosus Disease Activity Index 2000, SDI = Systemic Lupus International Collaborating Clinics/American College of Rheumatology Damage Index, DMARDs = Disease-modifying antirheumatic drugs, ANA = Antinuclear antibodies, Anti-dsDNA = Anti-double stranded DNA antibodies, Anti-Sm = Anti-Smith, aPL = Anti-phospholipid antibodies.

[a] Duration between SLE diagnosis and date of the MRI scan.

[b] Current or history of smoking.

[c] Positive serology in any of the following: Lupus Anticoagulant, anti-cardiolipin antibodies or anti-β2 glycoprotein I antibodies.

The frequency of NPSLE was 20%, 30%, and 59% when applying the SLICC A, SLICC B and NPACR models, respectively (Table 2). The most frequent NP manifestations according to the NPACR model were cognitive dysfunction (36 %), headache (31 %), autonomic neuropathy (16 %), depression (14 %) and anxiety (14 %). Autonomic and cranial neuropathy were most frequent when further applying the SLICC A and SLICC B models. Assessment of disease duration, SLEDAI-2 K and SDI in the NPSLE and non-NPSLE patients revealed no significant differences between the groups (data not shown).

3.2. Regional perfusion differences

The mean differences between the SLE patients and the HC group are presented in Fig. 3 and Supplementary Table 1. On average, 2.5 % increase in rCBF (range –23.2 – 28.3 %), 1.0 % decrease in rCBV (range −39.8 – 61.5 %) and 7.3 % decrease in rMTT (range −28.3 – 19.1 %) was found. After Bonferroni correction, the SLE cohort displayed significantly decreased rCBF in the pons, decreased rCBV in the bilateral putamina and posterior thalami, and decreased rMTT in the right anterior insula and bilaterally in the hypothalami, putamina and right posterior thalamus, compared to HC. Increased rCBF was present in the posterior corpus callosum and increased rCBV in the anterior corpus callosum, compared to HC. To investigate possible sex-related differences, we repeated the above-mentioned analysis with only female HC. Bilateral putamina in rCBV and the right anterior insula in rMTT showed a significant decrease in the regional perfusion after correction for multiple comparisons (Supplementary Table 2).

Table 2
NPSLE manifestations among the 64 patients in the SLE cohort, presented as number of patients (percentage of SLE patients), according to three NPSLE attribution models (SLICC A, SLICC B and NPACR).

		SLICC A	SLICC B	NPACR
Patients with NPSLE manifestations		13 (20 %)	19 (30 %)	38 (59 %)
CNS	Cognitive dysfunction	0 (0 %)	4 (6 %)	23 (36 %)
	Headache	N/A	N/A	20 (31 %)
	Depression	0 (0 %)	0 (0 %)	9 (14 %)
	Anxiety	N/A	N/A	9 (14 %)
	Cerebrovascular disease	1 (2 %)	4 (6 %)	4 (6 %)
	Acute confusion	1 (2 %)	2 (3 %)	3 (5 %)
	Demyelinating disease	2 (3 %)	2 (3 %)	2 (3 %)
	Epilepsy	1 (2 %)	1 (2 %)	1 (2 %)
	Psychosis	1 (2 %)	1 (2 %)	1 (2 %)
	Aseptic meningitis	1 (2 %)	1 (2 %)	1 (2 %)
	Chorea	0 (0 %)	1 (2 %)	1 (2 %)
	Myelopathy	0 (0 %)	1 (2 %)	1 (2 %)
PNS	Autonomic neuropathy	7 (11 %)	8 (13 %)	10 (16 %)
	Cranial neuropathy	5 (8 %)	5 (8 %)	5 (8 %)
	Mononeuropathy	1 (2 %)	2 (3 %)	2 (3 %)
	Polyneuropathy	1 (2 %)	1 (2 %)	2 (3 %)
	Plexopathy	0 (0 %)	0 (0 %)	0 (0 %)
	Guillain-Barré	0 (0 %)	0 (0 %)	0 (0 %)
	Myasthenia Gravis	0 (0 %)	0 (0 %)	0 (0 %)

A single patient might present with multiple manifestations, and the patients in SLICC A are by definition also included in SLICC B.
NPSLE = Neuropsychiatric systemic lupus erythematosus, SLICC = Systemic Lupus International Collaborating Clinics, NPACR = American College of Rheumatology case definitions for NPSLE, CNS = Central nervous system, PNS = Peripheral nervous system, N/A = Not applicable.

Comparisons between NPSLE and non-NPSLE patients revealed a general trend towards higher rCBF (mean increase 13.3 %) and rCBV (mean increase 13.9 %) using the SLICC A model, and a trend towards lower rMTT using the NPACR model (mean decrease 7.3 %) (Supplementary Table 3). No statistically significant perfusion differences were found in any of the ROIs, regardless of attribution model, after correction for multiple comparisons. When comparing NPSLE and non-NPSLE patients to HC, significant perfusion differences were found in the same areas for both NPSLE and non-NPSLE, using the SLICC A and SLICC B models. After correction for multiple comparisons, decreased rCBF was found in the pons, decreased rCBV in the right putamen and right posterior thalamus, and decreased rMTT in the right putamen and bilaterally in the hypothalami, compared to HC. When using the NPACR model significant results were found in the same areas, and, in addition, a significantly decreased rMTT in the right posterior thalamus and right anterior insula, compared to HC. The results are presented in Supplementary Table 4.

3.3. Perfusion and contrast leakage differences in WMHs compared to NAWM

Measurable WMHs were present in 31 SLE patients. Of these, 9, 12, and 16 patients were NPSLE patients when using the SLICC A, SLICC B, and NPACR attribution models, respectively. In general, the SLE patients had a WMH burden of 2 (range 1–25), WMH size of 0.074 ml/WMH (range 0.044–0.222 ml/WMH) and WMH volume of 0.192 ml/patient (range 0.044–3.062 ml/patient). Descriptive data regarding the WMHs are presented in Table 3. No significant differences in age or the WMH metrics were found between the NPSLE and non-NPSLE patients.

Significantly higher rCBF, rCBV, rMTT and K_2 were present in WMHs

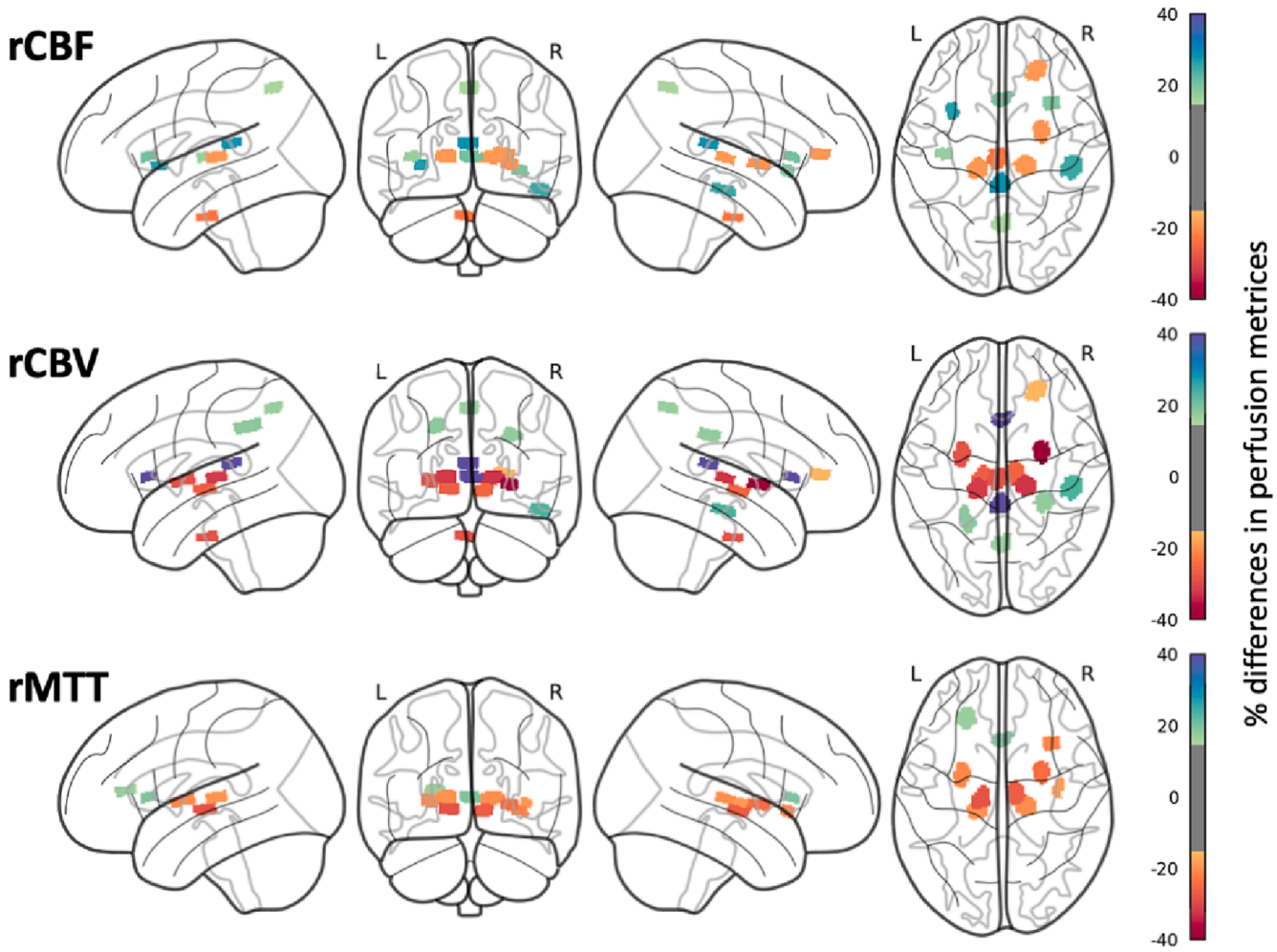

Fig. 3. Visualization of the perfusion differences in percentage between SLE and HC for rCBF (top), rCBV (middle) and rMTT (bottom). Only ROIs with a significant perfusion difference i.e., increases of more than 15 % and a decrease of more than −15 %, are shown. An overview of the exact percentages for each ROI can be found in Supplementary Table 1. ROI = Region of interest, SLE = Systemic lupus erythematosus, HC = Healthy Controls, rCBF = Relative cerebral blood flow, rCBV = Relative cerebral blood volume, rMTT = Mean transit time.

compared to NAWM in the SLE patients. The same significant pattern was found in all non-NPSLE groups regardless of the attribution model. NPSLE patients in the SLICC A and SLICC B models showed a significant increase in regional perfusion in WMHs compared to NAWM regarding rCBF, and in the NPACR model regarding rCBV. Higher K_2 was also found in all groups in WMHs compared to NAWM, and significantly among the non-NPSLE patients. The results in the SLE, NPSLE and non-NPSLE patients are presented in Table 3.

4. Discussion

This explorative study, using DSC-MRI, demonstrated abnormal cerebral perfusion in several areas of the brain in SLE patients compared to HC. In particular, we found a decrease in rMTT to be the most prevalent finding and it differed significantly in the right anterior insula, hypothalami, putamina as well as the right posterior thalamus. Previous findings of hypoperfusion in the thalami (Papadaki et al., 2018; Oda et al., 2005), insulae (Zhuo et al., 2020; Giovacchini et al., 2010) and basal ganglia (Papadaki et al., 2018; Papadaki et al., 2019; Zhang et al., 2005 Dec 15; Shen et al., 1999) suggest, in agreement with our results, that these areas could be affected in SLE patients. In addition to perfusion alterations, as measured with DSC-MRI, single-photon emission computed tomography (SPECT) and ASL, these areas further show potential involvement in SLE patients with altered microstructure on diffusion tensor imaging (DTI) as well as GM atrophy on conventional MRI (Hughes et al., 2007; Cagnoli et al., 2012). In contrast to a previous ASL study (Zhuo et al., 2020), we found decreased rCBF in the pons in SLE patients, which could reflect or predispose the presence of T2 hyperintensity lesions in the region (Abreu et al., 2005), and increased rCBF and rCBV in the corpus callosum. Our findings of decreased rCBV in the putamina and right posterior thalamus also contradicts some previous reports suggesting that SLE patients could have regional and even overall hyperperfusion compared to HC (Gasparovic et al., 2010; Wang et al., 2012). Together, this emphasizes that perfusion differences found with DSC-MRI and other imaging techniques in SLE patients are still inconclusively explored. However, our findings are expected to further the general knowledge in the field rather than contributing to individualized clinical practice at this point. The results confirm that SLE patients differ from HC also regarding perfusion metrics, and contribute to a better understanding of NPSLE pathogenetic mechanisms and how they are reflected in the CNS. Perfusion MRI measurements may contribute to individual assessments of SLE patients in the NPSLE context.

The MTT value can be described using the central volume theorem, stating that the MTT is given by the ratio CBV/CBF. Therefore, either an abnormal relative decrease in rCBV or an increase in rCBF (or both these effects) would result in a decreased rMTT. Interestingly, we found several regions that followed this pattern leading to a decreased rMTT,

Table 3
Descriptive WMH data for the SLE group and the SLICC A, SLICC B and NPACR groups. The differences in rCBF, rCBV, rMTT and K_2 are presented as the mean increase in percent in WMHs relative to NAWM. Values shown in bold were statistically significant ($p < 0.05$).

	SLE	SLICC A		SLICC B		NPACR	
		NPSLE	non-NPSLE	NPSLE	non-NPSLE	NPSLE	non-NPSLE
Patients with WMHs, n (%)[1]	31 (48 %)	9 (69 %)	22 (43 %)	12 (63 %)	19 (42 %)	16 (42 %)	15 (58 %)
Age [years], median (range)	41 (20–52)	41 (28–48)	41 (20–52)	40.5 (23–48)	43 (20–52)	41 (23–48)	42 (20–52)
WMH burden [n/patient], median (range)[2]	2 (1–25)	2 (1–20)	2 (1–25)	2.5 (1–20)	2 (1–25)	2 (1–20)	2 (1–25)
WMH size [ml/WMH], median (range)[2]	0.074 (0.044–0.222)	0.074 (0.052–0.222)	0.081 (0.044–0.155)	0.073 (0.052–0.222)	0.091 (0.044–0.155)	0.073 (0.044–0.222)	0.096 (0.044–0.155)
WMH volume [ml/patient], median (range)[2]	0.192 (0.044–3.062)	0.163 (0.074–1.716)	0.222 (0.044–3.062)	0.192 (0.059–1.716)	0.192 (0.044–3.062)	0.178 (0.044–1.716)	0.251 (0.044–3.062)
	WMH vs NAWM[3]						
rCBF, % (p value)	**39.1 % (<0.001)**	**48.2 % (0.021)**	**35.3 % (<0.001)**	**39.6 % (0.03)**	**38.8 % (<0.001)**	28.5 % (0.07)	**50.6 % (<0.001)**
rCBV, % (p value)	**69.0 % (<0.001)**	56.7 % (0.052)	**74.5 % (<0.001)**	54.2 % (0.053)	**78.1 % (0.001)**	**47.8 % (0.04)**	**90.5 % (<0.001)**
rMTT, % (p value)	**21.4 % (0.005)**	5.6 % (0.6)	**28.2 % (0.006)**	11.6 % (0.4)	**27.6 % (0.008)**	15.5 % (0.07)	**27.2 % (0.02)**
K2, % (p value)	**231.4% (<0.001)**	119.1 % (0.2)	**273.7 % (<0.001)**	87.0 % (0.2)	**358.1 % (<0.001)**	126.7 % (0.1)	**385 % (<0.001)**

SLE = Systemic lupus erythematosus, NPSLE = Neuropsychiatric SLE, SLICC = Systemic Lupus International Collaborating Clinics, NPACR = American College of Rheumatology case definitions for NPSLE, WMH(s) = White matter hyperintensity(s), NAWM = Normal appearing white matter, rCBF = Relative cerebral blood flow, rCBV = Relative cerebral blood volume, rMTT = Relative mean transit time, K_2 = Blood-brain barrier leakage parameter.
[1] The number and percentage of patients in the respective group (SLE, SLICC A, SLICC B, NPACR) that presented with measurable WMHs.
[2] Based on the regions of interest which were placed in the perfusion weighted images (defined as 3 pixels or volume $\geq$ 0.044 ml).
[3] The mean increase in percent in the WMHs relative to NAWM, calculated as ((WMH/NAWM) − 1) × 100.

some of which were significant after correction for multiple comparisons, as presented in Supplementary Table 1. While a reduction in rMTT is not often reported in the literature, it has been hypothesized that a shortened rMTT in acute stroke could be due to errors attributed to the SVD deconvolution when there is poor collateral circulation and restricted diffusion or blood flow (Doucet et al., 2016; Murayama et al., 2017; Dababneh et al., 2011). However, the importance and interpretation of these findings in the context of SLE remains to be further evaluated, as to the best of our knowledge, no previous DSC-MRI research has found any rMTT differences between SLE patients and HC (Papadaki et al., 2018; Wang et al., 2012; Emmer et al., 2010).

Correct diagnosis of NPSLE is still a clinical challenge, and difficulties may arise when determining whether previous and ongoing NP symptoms are primarily caused by SLE, secondary to unrelated causes (such as infections or medications) or due to comorbidities (Bortoluzzi et al., 2018). Thus, different more or less stringent attribution models have been developed, and to our knowledge, this is the first work to use the more stringent SLICC A and SLICC B models alongside the NPACR model to evaluate cerebral perfusion in NPSLE and non-NPSLE patients. We found that none of the investigated metrics revealed any significant differences, in concordance with some previous DSC-MRI studies that also were unable to distinguish the patients (Papadaki et al., 2019; Wang et al., 2012; Emmer et al., 2010; Zimny et al., 2014). This could be an expression of the variability in perfusion-based values among the patient groups, and the heterogeneity of the clinical phenotypes, including the possibility of subclinical NP involvement among patients labeled as non-NPSLE within the current definitions (Wang et al., 2012; Bortoluzzi et al., 2018 Mar). Additionally, as a consequence of the consecutive recruitment of patients, NP manifestations in the NPSLE patient groups were in general not acute onset nor necessarily active despite ongoing symptoms. We emphasize that other study designs are needed to specifically evaluate SLE patients with acute onset or ongoing NP involvement related to cerebral perfusion.

Interestingly, we demonstrated significant alterations in the perfusion-based metrics for both NPSLE patients and non-NPSLE patients when compared with HC. These results are in agreement with the findings in the general SLE group, and suggest that SLE patients, independently of NP involvement, might present with altered cerebral perfusion compared to HC. A decrease in rCBV has previously been reported in the thalami and lenticular nuclei in NPSLE patients compared to HC (Papadaki et al., 2018), which is in line with our findings of reduced rCBV in the same areas, and particularly in the' right putamen and right posterior thalamus after correcting for multiple comparisons. Even in non-NPSLE patients, these regions, which are part of the cortico-basal ganglia-thalamic-cortical circuit, have shown decreased signaling on blood oxygenation level-dependent (BOLD) functional MRI (fMRI), which has been hypothesized to cause impairment of both response control and behavioral change (Ren et al., 2012). Furthermore, a previous study, using quantitative susceptibility mapping (QSM), demonstrated iron accumulation in the putamina in NPSLE patients compared to both non-NPSLE patients and HC (Ogasawara et al., 2016). These findings, potentially caused by underlying neuroinflammation, are suggested to further underestimate the perfusion values in this area (Yamada et al., 2002). Although a later study was unable to replicate these changes (Bulk et al., 2021), a possible iron-induced susceptibility effect should, still, be considered. While no obvious calcifications were seen in the basal ganglia in our SLE cohort, the inconclusive results from previous studies concerning iron accumulation (Ogasawara et al., 2016; Bulk et al., 2021) warrant the inclusion of QSM in future SLE studies.

WMHs seen on T2-weighted FLAIR images have been proposed to be caused by a variety of different factors in SLE patients (Ota et al., 2022; Luyendijk et al., 2011; Shaharir et al., 2018), and our secondary aim included investigating the vascular properties of these hyperintensities with DSC-MRI. We found significantly increased values for all perfusion-based measurements (rCBF, rCBV and rMTT) in WMHs compared to NAWM in the SLE cohort, indicating hyperperfusion and a relatively higher increase in rCBV compared to rCBF, as required for an observation of increased rMTT. These results are in agreement with previous studies in healthy individuals showing a higher rMTT in WMHs compared to NAWM (Dewey et al., 2021; Marstrand et al., 2002), but are in contrast to reports of reduced rCBF (Marstrand et al., 2002; Brickman et al., 2009; Promjunyakul et al., 2015) and rCBV (Sachdev et al., 2004) in the tissue surrounding WMHs, also found for SLE patients (Gasparovic et al., 2010). While these prior findings could be related to small vessel disease or ischemia, which are possible factors contributing to WMH load (Luyendijk et al., 2011; Shaharir et al., 2018; Magro Checa et al., 2013 Jun), few studies have specifically investigated perfusion-based metrics in WMHs in SLE. However, hyperintensity lesions in the context of multiple sclerosis (MS) have been reported to show increased CBF and CBV compared to NAWM, related to contrast enhancement as

an expression of inflammatory activity (Lapointe et al., 2018; Yin et al., 2018). Although WMHs in SLE often have different characteristics on conventional MRI compared to those seen in MS, SLE patients could also present with demyelinating disease as an NP event, complicating the diagnosis (Magro Checa et al., 2013 Jun). Given the non-specific nature of WMHs in SLE (Ota et al., 2022; Jennings et al., 2004; Luyendijk et al., 2011), our findings raise the possibility of inflammation with vasodilation rather than ischemia, highlighting the importance of further research to provide nuance and additional knowledge.

In addition, we also found K_2 to be increased in WMHs compared to NAWM in the SLE cohort, which reflects the level of contrast agent leakage into the extravascular extracellular space and would be an indicator of a compromised BBB. This study is, to our knowledge, the first to investigate the BBB using K_2 specifically in WMHs for SLE patients. Previous research has used DCE-MRI and found the permeability weighted volume transfer constant (K^{trans}) to be increased in SLE compared to HC, while utilizing an explorative method of ROI placement in certain brain regions (Chi et al., 2019; Kamintsky et al., 2020). Since we measured K_2 in absolute values without normalization, we decided it was most suitable to compare differences between WMHs and NAWM within the SLE group and not compared to HC. Our results support the hypothesis of BBB dysfunction as part of the vascular pathology and potential WMH formation in SLE patients (Stock et al., 2017). This increase in BBB permeability is also consistent with DCE-MRI research in healthy individuals (Dewey et al., 2021), MS patients with active lesions (Yin et al., 2018) and cerebral small vessel disease (Huisa et al., 2015; Wong et al., 2019), where similar results have been found indicating a disruption of the BBB in different WMHs compared to NAWM. Our and others' findings suggest that K_2 should be of value, especially when used in tandem with K^{trans} and measurements of cerebral perfusion, to investigate the integrity of the BBB related to vasodilation, and possibly affected by neuroinflammation in SLE patients (Nikolopoulos et al., 2019; Stock et al., 2017).

This study is not without limitations. The perfusion values could be affected by PVEs due to the DSC-MRI spatial resolution, which might include surrounding tissue in the ROIs. However, in order to minimize these effects, we placed each ROI carefully and with guidance of the higher spatial resolution of the FLAIR and MPRAGE images. Additional consideration was given to the WMHs, where hyperintensities smaller than 3 pixels (volume $<$0.044 ml) were excluded for this reason. Normalizing the perfusion values to a reference region reduces PVE related errors in the quantification (Jafari-Khouzani et al., 2015) but introduces the assumption that a certain brain region is unaffected by SLE. The middle cerebellar peduncle has previously been used with the motivation of being less often affected (Papadaki et al., 2018; Papadaki et al., 2019), and we wanted to use a similar approach. However, the overall lack of a common denominator in the literature (Gasparovic et al., 2010; Wang et al., 2012; Emmer et al., 2010; Zimny et al., 2014) could influence the comparability to other DSC-MRI studies in SLE. Another study limitation is the use of different scanners and imaging protocols for the SLE and HC cohorts. While the 90° flip angle might increase the T1 effects in the acquired DSC images for the SLE cohort, the use of a longer TR, as well as normalization of the perfusion-based values, reduces the sensitivity to any dissimilarities related to different settings in the image acquisition (Jafari-Khouzani et al., 2015; Semmineh et al., 2018). Furthermore, quantification of K_2 can be hampered by arrival time delay and an additional correction method could be used in future studies (Leigh et al., 2012).

Finally, the conclusions may be hampered by the sample sizes of the study groups, although our overall SLE cohort is larger than most previous DSC-MRI studies (Borrelli et al., 2003; Gasparovic et al., 2010; Wang et al., 2012; Emmer et al., 2010; Zimny et al., 2014). However, larger sample sizes would allow for the analysis of additional subgroups, for example, evaluation of the perfusion based on specific NP manifestations and with different SLE disease activity in general. This could potentially gain further insight into the vascular pathophysiology behind the different phenotypes of NP involvement in SLE. In our cohort the patients had no or low ongoing SLE activity, and any immunosuppressive treatment may have influenced the results, in particular, by potentially reducing pathological findings. A larger sample size would also allow the inclusion of all sexes. Although SLE is a disease most commonly seen in females (Unterman et al., 2011), a generalization of our results should be avoided. Even if a small majority of the HC were female, there was indeed a difference in male-female composition between the SLE and HC groups. Besides previously documented differences in perfusion values between men and women using DSC-MRI (Shin et al., 2007), when removing the male HC in our analysis a similar pattern in all perfusion metrics was obtained in the all-female control group compared to the whole HC group. The general direction of increases and decreases in the regional perfusion ROIs compared to SLE remained consistent. However, significances in the perfusion metrics were reduced, mostly due to a decreased statistical power.

5. Conclusion

This study used DSC-MRI to demonstrate significant alterations in cerebral perfusion in female SLE patients with and without NP involvement, regardless of NPSLE attribution model, compared to HC. WMHs showed significantly increased rCBF, rCBV, rMTT and K_2 compared to NAWM in the SLE cohort. These findings provide additional insight into the role of BBB dysfunction and the vascular properties of WMHs in female SLE patients. Despite the disease being most frequent in females, generalization of our conclusions to SLE patients overall should be avoided. Several brain regions could be of interest in SLE, and further prospective well-regulated studies, evaluating cerebral perfusion and its clinical impact on the disease, need to be conducted.

CRediT authorship contribution statement

T. Salomonsson: Writing – original draft, Investigation, Data curation, Formal analysis, Visualization. **T. Rumetshofer:** Writing – original draft, Methodology, Investigation, Data curation, Formal analysis, Software, Visualization. **A. Jönsen:** Conceptualization, Methodology, Data curation, Resources, Writing – review & editing. **A.A. Bengtsson:** Conceptualization, Resources, Writing – review & editing. **K.A. Zervides:** Investigation, Data curation, Writing – review & editing. **P. Nilsson:** Investigation, Resources, Writing – review & editing. **M. Knutsson:** Investigation, Data curation, Formal analysis. **R. Wirestam:** Funding acquisition, Methodology, Writing – review & editing. **J. Lätt:** Software, Resources, Data curation, Writing – review & editing. **L. Knutsson:** Conceptualization, Methodology, Data curation, Funding acquisition, Resources, Writing – original draft. **P.C. Sundgren:** Conceptualization, Methodology, Project administration, Funding acquisition, Resources, Supervision, Writing – review & editing.

Declaration of Competing Interest

The authors declare that they have no known competing financial interests or personal relationships that could have appeared to influence the work reported in this paper.

Data availability

Data will be made available on request.

Acknowledgement

The authors would also like to thank Markus Nilsson for providing the software Eval GUI used in the analysis.

Funding

This study was supported by funding from Gustav V 80-years foundation (FAI2017-0341), Skåne University Hospital Research Funding (2017-2021), Swedish Rheumatism Association (R-568371), Alfred Österlunds Research Foundation, Greta and Johan Kocks Foundation (2015-2016), Swedish Research Foundation (2017-00995) and the Swedish Brain Foundation (FO2018-0145).

The funding sources had no involvement in the study design, in the collection, analysis and interpretation of data, in the writing of the report and in the decision to submit the article for publication.

Appendix A. Supplementary data

Supplementary data to this article can be found online at https://doi.org/10.1016/j.nicl.2023.103390.

References

Abreu, M.R., Jakosky, A., Folgerini, M., Brenol, J.C.T., Xavier, R.M., Kapczinsky, F., 2005. Neuropsychiatric systemic lupus erythematosus: correlation of brain MR imaging, CT, and SPECT. Clin Imaging. 29 (3), 215–221.

Ainiala, H., Hietaharju, A., Loukkola, J., Peltola, J., Korpela, M., Metsänoja, R., Auvinen, A., 2001. Validity of the new American College of Rheumatology criteria for neuropsychiatric lupus syndromes: a population-based evaluation. Arthritis Rheum. 45 (5), 419–423.

Borrelli, M., Tamarozzi, R., Colamussi, P., Govoni, M., Trotta, F., Lappi, S., 2003. Evaluation with MR, perfusion MR and cerebral flowSPECT in NPSLE patients. Radiol Med. 105 (5–6), 482–489.

Bortoluzzi, A., Scirè, C.A., Govoni, M., 2018. Attribution of neuropsychiatric manifestations to systemic lupus erythematosus. Front Med (Lausanne). 14 (5), 68.

Boxerman, J.L., Schmainda, K.M., Weisskoff, R.M., 2006. Relative cerebral blood volume maps corrected for contrast agent extravasation significantly correlate with glioma tumor grade, whereas uncorrected maps do not. AJNR Am J Neuroradiol. 27 (4), 859–867.

Brickman, A.M., Zahra, A., Muraskin, J., Steffener, J., Holland, C.M., Habeck, C., Borogovac, A., Ramos, M.A., Brown, T.R., Asllani, I., Stern, Y., 2009. Reduction in cerebral blood flow in areas appearing as white matter hyperintensities on magnetic resonance imaging. Psychiatry Res. 172 (2), 117–120.

Bulk, M., van Harten, T., Kenkhuis, B., Inglese, F., Hegeman, I., van Duinen, S., Ercan, E., Magro-Checa, C., Goeman, J., Mawrin, C., van Buchem, M., Steup-Beekman, G., Huizinga, T., van der Weerd, L., Ronen, I., 2021. Quantitative susceptibility mapping in the thalamus and basal ganglia of systemic lupus erythematosus patients with neuropsychiatric complaints. Neuroimage Clin. 30.

Cagnoli, P.C., Sundgren, P.C., Kairys, ANSON, Graft, C.C., Clauw, D.J., Gebarski, STEPHEN, McCUNE, W.J., Schmidt-wilcke, TOBIAS, 2012. Changes in regional brain morphology in neuropsychiatric systemic lupus erythematosus. J Rheumatol. 39 (5), 959–967.

Chi, J.M., Mackay, M., Hoang, A., Cheng, K., Aranow, C., Ivanidze, J., et al., 2019. Alterations in Blood-Brain Barrier Permeability in Patients with Systemic Lupus Erythematosus. AJNR Am J Neuroradiol. 40 (3), 470–477.

Dababneh, H., Guerrero, W., Wilson, K., Mocco, J.D., 2011. Observation of Mean Transit Time (Mtt) Perfusion Maps on a 320-Detector Row Ct Scanner and its Potential Application in Acute Ischemic Stroke. J Neurol Neurophysiol. 02 (04).

Dewey, B.E., Xu, X., Knutsson, L., Jog, A., Prince, J.L., Barker, P.B., van Zijl, P.C.M., Leigh, R., Nyquist, P., 2021. MTT and Blood-Brain Barrier Disruption within Asymptomatic Vascular WM Lesions. AJNR Am J Neuroradiol 42 (8), 1396–1402.

Doucet, C., Roncarolo, F., Tampieri, D., Del Pilar, C.M., 2016. Paradoxically decreased mean transit time in patients presenting with acute stroke. J Comput Assist Tomogr. 40 (3), 409–412.

Emmer, B.J., van Osch, M.J., Wu, O., Steup-Beekman, G.M., Steens, S.C., Huizinga, T.W., van Buchem, M.A., van der Grond, J., 2010. Perfusion MRI in neuro-psychiatric systemic lupus erthemathosus. J Magn Reson Imaging. 32 (2), 283–288.

Fisel, C.R., Ackerman, J.L., Buxton, R.B., Garrido, L., Belliveau, J.W., Rosen, B.R., Brady, T.J., 1991. MR contrast due to microscopically heterogeneous magnetic susceptibility: numerical simulations and applications to cerebral physiology. Magn Reson Med. 17 (2), 336–347.

Gasparovic, C.M., Roldan, C.A., Sibbitt, W.L., Qualls, C.R., Mullins, P.G., Sharrar, J.M., Yamamoto, J.J., Bockholt, H.J., 2010. Elevated cerebral blood flow and volume in systemic lupus measured by dynamic susceptibility contrast magnetic resonance imaging. J Rheumatol. 37 (9), 1834–1843.

Giovacchini, GIAMPIERO, Mosca, MARTA, Manca, GIANPIERO, Della porta, MAURO, Neri, CLAUDIA, Bombardieri, STEFANO, Ciarmiello, ANDREA, Strauss, H.W., Mariani, GIULIANO, Volterrani, DUCCIO, 2010. Cerebral blood flow in depressed patients with systemic lupus erythematosus. J Rheumatol. 37 (9), 1844–1851.

Gladman, D., Ginzler, E., Goldsmith, C., Fortin, P., Liang, M., Sanchez-Guerrero, J., Urowitz, M., Bacon, P., Bombardieri, S., Hanly, J., Jones, J., Hay, E., Symmons, D., Isenberg, D., Kalunion, K., Maddison, P., Nived, O., Sturfelt, G., Petri, M., Richter, M., Snaith, M., Zoma, A., 1996. The development and initial validation of the Systemic Lupus International Collaborating Clinics/American College of Rheumatology damage index for systemic lupus erythematosus. Arthritis Rheum. 39 (3), 363–369.

Gladman, D.D., Ibañez, D., Urowitz, M.B., 2002. Systemic lupus erythematosus disease activity index 2000. J Rheumatol. 29 (2), 288–291.

Hanly, J.G., McCurdy, G., Fougere, L., Douglas, J.-A., Thompson, K., 2004. Neuropsychiatric events in systemic lupus erythematosus: attribution and clinical significance. J Rheumatol. 31 (11), 2156–2162.

Hanly, J.G., Urowitz, M.B., Sanchez-Guerrero, J., Bae, S.C., Gordon, C., Wallace, D.J., Isenberg, D., Alarcón, G.S., Clarke, A., Bernatsky, S., Merrill, J.T., Petri, M., Dooley, M.A., Gladman, D., Fortin, P.R., Steinsson, K., Bruce, I., Manzi, S., Khamashta, M., Zoma, A., Aranow, C., Ginzler, E., Van Vollenhoven, R., Font, J., Sturfelt, G., Nived, O., Ramsey-Goldman, R., Kalunian, K., Douglas, J., Thompson, K., Farewell, V., 2007. Neuropsychiatric events at the time of diagnosis of systemic lupus erythematosus: an international inception cohort study. Arthritis Rheum. 56 (1), 265–273.

Hanly, J.G., Urowitz, M.B., Su, L., Sanchez-Guerrero, J., Bae, S.C., Gordon, C., Wallace, D.J., Isenberg, D., Alarcón, G.S., Merrill, J.T., Clarke, A., Bernatsky, S., Dooley, M.A., Fortin, P.R., Gladman, D., Steinsson, K., Petri, M., Bruce, I.N., Manzi, S., Khamashta, M., Zoma, A., Font, J., Van Vollenhoven, R., Aranow, C., Ginzler, E., Nived, O., Sturfelt, G., Ramsey-goldman, R., Kalunian, K., Douglas, J., Qiufen Qi, K., Thompson, K., Farewell, V., 2008. Short-term outcome of neuropsychiatric events in systemic lupus erythematosus upon enrollment into an international inception cohort study. Arthritis Rheum. 59 (5), 721–729.

Hughes, M., Sundgren, P.C., Fan, X., Foerster, B., Nan, B., Welsh, R.C., Williamson, J.A., Attwood, J., Maly, P.V., Chenevert, T.L., McCune, W., Gebarski, S., 2007. Diffusion tensor imaging in patients with acute onset of neuropsychiatric systemic lupus erythematosus: a prospective study of apparent diffusion coefficient, fractional anisotropy values, and eigenvalues in different regions of the brain. Acta Radiol. 48 (2), 213–222.

Huisa, B.N., Caprihan, A., Thompson, J., Prestopnik, J., Qualls, C.R., Rosenberg, G.A., 2015. Long-Term Blood-Brain Barrier Permeability Changes in Binswanger Disease. Stroke. 46 (9), 2413–2418.

Jafari-Khouzani, K., Emblem, K.E., Kalpathy-Cramer, J., Bjørnerud, A., Vangel, M.G., Gerstner, E.R., Schmainda, K.M., Paynabar, K., Wu, O., Wen, P.Y., Batchelor, T., Rosen, B., Stufflebeam, S.M., 2015. Repeatability of cerebral perfusion using dynamic susceptibility contrast MRI in glioblastoma patients. Transl Oncol. 8 (3), 137–146.

Jenkinson, M., Bannister, P., Brady, M., Smith, S., 2002. Improved optimization for the robust and accurate linear registration and motion correction of brain images. Neuroimage. 17 (2), 825–841.

Jenkinson, M., Smith, S., 2001. A global optimisation method for robust affine registration of brain images. Med Image Anal. 5 (2), 143–156.

Jennings, J.E., Sundgren, P.C., Attwood, J., McCune, J., Maly, P., 2004. Value of MRI of the brain in patients with systemic lupus erythematosus and neurologic disturbance. Neuroradiology. 46 (1), 15–21.

Jia, J., Xie, J., Li, H., Wei, H., Li, X., Hu, J., Meng, D., Zhang, Y., Zhang, X., 2019. Cerebral blood flow abnormalities in neuropsychiatric systemic lupus erythematosus. Lupus. 28 (9), 1128–1133.

Kamintsky, L., Beyea, S.D., Fisk, J.D., Hashmi, J.A., Omisade, A., Calkin, C., Bardouille, T., Bowen, C., Quraan, M., Mitnitski, A., Matheson, K., Friedman, A., Hanly, J.G., 2020. Blood-brain barrier leakage in systemic lupus erythematosus is associated with gray matter loss and cognitive impairment. Ann Rheum Dis. 79 (12), 1580–1587.

Knutsson, L., Lindgren, E., Ahlgren, A., van Osch, M.J.P., Bloch, K.M., Surova, Y., Ståhlberg, F., van Westen, D., Wirestam, R., 2014. Dynamic susceptibility contrast MRI with a prebolus contrast agent administration design for improved absolute quantification of perfusion. Magn Reson Med. 72 (4), 996–1006.

Lapointe, E., Li, D.K.B., Traboulsee, A.L., Rauscher, A., 2018. What Have We Learned from Perfusion MRI in Multiple Sclerosis? AJNR Am J Neuroradiol. 39 (6), 994–1000.

Leigh, R., Jen, S.S., Varma, D.D., Hillis, A.E., Barker, P.B., Herholz, K., 2012. Arrival time correction for dynamic susceptibility contrast MR permeability imaging in stroke patients. PLoS ONE. 7 (12).

Luyendijk, J., Steens, S.C.A., Ouwendijk, W.J.N., Steup-Beekman, G.M., Bollen, E.L.E.M., van der Grond, J., Huizinga, T.W.J., Emmer, B.J., van Buchem, M.A., 2011. Neuropsychiatric systemic lupus erythematosus: lessons learned from magnetic resonance imaging. Arthritis Rheum. 63 (3), 722–732.

Magro Checa, C., Cohen, D., Bollen, E.L.E.M., van Buchem, M.A., Huizinga, T.W.J., Steup-Beekman, G.M., 2013. Demyelinating disease in SLE: is it multiple sclerosis or lupus? Best Pract Res Clin Rheumatol. 27 (3), 405–424.

Marstrand, J.R., Garde, E., Rostrup, E., Ring, P., Rosenbaum, S., Mortensen, E.L., Larsson, H.B.W., 2002. Cerebral perfusion and cerebrovascular reactivity are reduced in white matter hyperintensities. Stroke. 33 (4), 972–976.

Murayama, K., Katada, K., Hayakawa, M., Toyama, H., 2017. Shortened mean transit time in CT perfusion with singular value decomposition analysis in acute cerebral infarction: quantitative evaluation and comparison with various CT perfusion parameters. J Comput Assist Tomogr. 41 (2), 173–180.

Nikolopoulos, D., Fanouriakis, A., Boumpas, D.T., 2019. Update on the pathogenesis of central nervous system lupus. Curr Opin Rheumatol. 31 (6), 669–677.

Oda, K., Matsushima, E., Okubo, Y., Ohta, K., Murata, Y., Koike, R., Miyasaka, N., Kato, M., 2005. Abnormal regional cerebral blood flow in systemic lupus erythematosus patients with psychiatric symptoms. J Clin Psychiatry. 66 (07), 907–913.

Ogasawara, A., Kakeda, S., Watanabe, K., Ide, S., Ueda, I., Murakami, Y.u., Moriya, J., Futatsuya, K., Sato, T., Nakayamada, S., Saito, K., Tanaka, Y., Liu, T., Wang, Y.i., Korogi, Y., 2016. Quantitative susceptibility mapping in patients with systemic lupus

erythematosus: detection of abnormalities in normal-appearing basal ganglia. Eur Radiol. 26 (4), 1056–1063.
Ota, Y., Srinivasan, A., Capizzano, A.A., Bapuraj, J.R., Kim, J., Kurokawa, R., Baba, A., Moritani, T., 2022. Central nervous system systemic lupus erythematosus: pathophysiologic, clinical, and imaging features. Radiographics 42 (1), 212–232.
Papadaki, E., Fanouriakis, A., Kavroulakis, E., Karageorgou, D., Sidiropoulos, P., Bertsias, G., Simos, P., Boumpas, D.T., 2018. Neuropsychiatric lupus or not? Cerebral hypoperfusion by perfusion-weighted MRI in normal-appearing white matter in primary neuropsychiatric lupus erythematosus. Ann Rheum Dis. 77 (3), 441–448.
Papadaki, E., Kavroulakis, E., Bertsias, G., Fanouriakis, A., Karageorgou, D., Sidiropoulos, P., Papastefanakis, E., Boumpas, D.T., Simos, P., 2019. Regional cerebral perfusion correlates with anxiety in neuropsychiatric SLE: evidence for a mechanism distinct from depression. Lupus. 28 (14), 1678–1689.
Petri, M., Orbai, A.-M., Alarcón, G.S., Gordon, C., Merrill, J.T., Fortin, P.R., et al., 2012. Derivation and validation of the Systemic Lupus International Collaborating Clinics classification criteria for systemic lupus erythematosus. Arthritis Rheum. 64 (8), 2677–2686.
Promjunyakul, N., Lahna, D., Kaye, J.A., Dodge, H.H., Erten-Lyons, D., Rooney, W.D., Silbert, L.C., 2015. Characterizing the white matter hyperintensity penumbra with cerebral blood flow measures. Neuroimage Clin. 8, 224–229.
Ren, T., Ho, R.-C.-M., Mak, A., 2012. Dysfunctional cortico-basal ganglia-thalamic circuit and altered hippocampal-amygdala activity on cognitive set-shifting in non-neuropsychiatric systemic lupus erythematosus. Arthritis Rheum. 64 (12), 4048–4059.
Sachdev, P., Wen, W., Shnier, R., Brodaty, H., 2004. Cerebral blood volume in T2-weighted white matter hyperintensities using exogenous contrast based perfusion MRI. J Neuropsychiatry Clin Neurosci. 16 (1), 83–92.
Semmineh, N.B., Bell, L.C., Stokes, A.M., Hu, L.S., Boxerman, J.L., Quarles, C.C., 2018. Optimization of Acquisition and Analysis Methods for Clinical Dynamic Susceptibility Contrast MRI Using a Population-Based Digital Reference Object. AJNR Am J Neuroradiol. 39 (11), 1981–1988.
Shaharir, S.S., Osman, S.S., Md Rani, S.A., Sakthiswary, R., Said, M.S.M., 2018. Factors associated with increased white matter hyperintense lesion (WMHI) load in patients with systemic lupus erythematosus (SLE). Lupus. 27 (1), 25–32.
Shen, Y.Y., Kao, C.H., Ho, Y.J., Lee, J.K., 1999. Regional cerebral blood flow in patients with systemic lupus erythematosus. J Neuroimaging. 9 (3), 160–164.
Shin, W., Horowitz, S., Ragin, A., Chen, Y., Walker, M., Carroll, T.J., 2007. Quantitative cerebral perfusion using dynamic susceptibility contrast MRI: evaluation of reproducibility and age- and gender-dependence with fully automatic image postprocessing algorithm. Magn Reson Med. 58 (6), 1232–1241.
Smith, S.M., 2002. Fast robust automated brain extraction. Hum Brain Mapp. 17 (3), 143–155.
Stock, A.D., Gelb, S., Pasternak, O., Ben-Zvi, A., Putterman, C., 2017. The blood brain barrier and neuropsychiatric lupus: new perspectives in light of advances in understanding the neuroimmune interface. Autoimmun Rev. 16 (6), 612–619.
The American College of Rheumatology nomenclature and case definitions for neuropsychiatric lupus syndromes. Arthritis Rheum. 1999 Apr. 42 (4). 599–608.
Unterman, A., Nolte, J.E.S., Boaz, M., Abady, M., Shoenfeld, Y., Zandman-Goddard, G., 2011. Neuropsychiatric syndromes in systemic lupus erythematosus: a meta-analysis. Semin Arthritis Rheum. 41 (1), 1–11.
Virtanen, P., Gommers, R., Oliphant, T.E., Haberland, M., Reddy, T., Cournapeau, D., et al., 2020. SciPy 1.0: fundamental algorithms for scientific computing in Python. Nat Methods. 17 (3), 261–272.
Wang, P.I., Cagnoli, P.C., McCune, W.J., Schmidt-Wilcke, T., Lowe, S.E., Graft, C.C., Gebarski, S.S., Chenevert, T.L., Khalatbari, S., Myles, J.D., Watcharotone, K., Cronin, P., Sundgren, P.C., 2012. Perfusion-weighted MR Imaging in Cerebral Lupus Erythematosus. Acad Radiol. 19 (8), 965–970.
Wong, S.M., Jansen, J.F.A., Zhang, C.E., Hoff, E.I., Staals, J., van Oostenbrugge, R.J., Backes, W.H., 2019. Blood-brain barrier impairment and hypoperfusion are linked in cerebral small vessel disease. Neurology. 92 (15), e1669 e1677.
Wu, O., Østergaard, L., Weisskoff, R.M., Benner, T., Rosen, B.R., Sorensen, A.G., 2003. Tracer arrival timing-insensitive technique for estimating flow in MR perfusion-weighted imaging using singular value decomposition with a block-circulant deconvolution matrix. Magn Reson Med. 50 (1), 164–174.
Yamada, K., Gonzalez, R.G., ØStergaard, L., Komili, S., Weisskoff, R.M., Rosen, B.R., et al., 2002. Iron-induced susceptibility effect at the globus pallidus causes underestimation of flow and volume on dynamic susceptibility contrast-enhanced MR perfusion images. AJNR Am J Neuroradiol. 23 (6), 1022–1029.
Yin, P., Xiong, H., Liu, Y.i., Sah, ShambhuK, Zeng, C., Wang, J., Li, Y., Hong, N., 2018. Measurement of the permeability, perfusion, and histogram characteristics in relapsing-remitting multiple sclerosis using dynamic contrast-enhanced MRI with extended Tofts linear model. Neurol India. 66 (3), 709.
Zhang, X., Zhu, Z., Zhang, F., Shu, H., Li, F., Dong, Y., 2005 Dec 15. Diagnostic value of single-photon-emission computed tomography in severe central nervous system involvement of systemic lupus erythematosus: a case-control study. Arthritis Rheum. 53 (6), 845–849.
Zhuo, Z., Su, L.i., Duan, Y., Huang, J., Qiu, X., Haller, S., Li, H., Zeng, X., Liu, Y., 2020. Different patterns of cerebral perfusion in SLE patients with and without neuropsychiatric manifestations. Hum Brain Mapp. 41 (3), 755–766.
Zimny, A., Szmyrka-Kaczmarek, M., Szewczyk, P., Bladowska, J., Pokryszko-Dragan, A., Gruszka, E., et al., 2014. In vivo evaluation of brain damage in the course of systemic lupus erythematosus using magnetic resonance spectroscopy, perfusion-weighted and diffusion-tensor imaging. Lupus. 23 (1), 10–19.